Proc. Natl. Acad. Sci. USA
Vol. 90, pp. 11965–11969, December 1993
Medical Sciences

Single photon emission computed tomographic imaging demonstrates loss of striatal dopamine transporters in Parkinson disease

R. B. INNIS*, J. P. SEIBYL*, B. E. SCANLEY*, M. LARUELLE*, A. ABI-DARGHAM*, E. WALLACE*, R. M. BALDWIN*, Y. ZEA-PONCE*, S. ZOGHBI*, S. WANG†, Y. GAO†, J. L. NEUMEYER†, D. S. CHARNEY*, P. B. HOFFER*‡, AND K. L. MAREK*

*Departments of Psychiatry, Neurology, and Diagnostic Radiology, Yale University School of Medicine and Veterans Affairs Medical Center, West Haven, CT 06518; and †Research Biochemicals International, Natick, MA 01760

Communicated by Robert G. Shulman, August 16, 1993

ABSTRACT **[^{123}I][(1*R*)-2β-carbomethoxy-3β-(4-iodophenyl)tropane] ([^{123}I]β-CIT) labels dopamine transporters and is, therefore, a marker of neurons that degenerate in Parkinson disease. Single photon emission computed tomography imaging with [^{123}I]β-CIT showed that radioactivity in striatal regions in healthy subjects increased during a 2-day imaging study, whereas that in Parkinsonian patients peaked earlier at reduced levels relative to healthy subjects. Kinetic analyses of radioactivity in plasma and brain suggest that this decrease was due to an ≈65% loss of target sites in patients compared with healthy subjects; greater losses occurred in putamen than in caudate. All patients showed lateralized differences in striatal uptake, with greater losses in the striatum contralateral to the side of the body with initial symptoms. These preliminary results suggest that [^{123}I]β-CIT is a marker for the loss of striatal dopamine terminals in patients with Parkinson disease. Single photon emission computed tomographic imaging with [^{123}I]β-CIT may be useful for early diagnosis of the disorder, for monitoring the progression of the disease, and for distinguishing the idiopathic disorder from other Parkinsonian syndromes with more widespread pathology.**

Parkinson disease is a progressive, disabling neurodegenerative disorder characterized clinically by tremor at rest, bradykinesia, rigidity, and postural instability. The disorder is characterized pathologically by the degeneration of dopaminergic neurons in the substantia nigra, resulting in an 80–99% reduction in striatal dopamine concentrations (1) and a corresponding loss of dopamine transporters (2). Dopamine replacement with either the precursor L-dopa (L-dihydroxyphenylalanine) or direct dopamine-receptor agonists effectively reverses the motor deficits of the disease early in its course. However, as the disease progresses, patients develop disabilities from a number of drug-induced side effects, progression of motor dysfunction (due to continued degeneration of dopamine nerve terminals), and an array of nonmotor, non-dopamine responsive symptoms. Therefore, recent research has focused on developing therapeutic strategies to prevent progression of disease by halting neuronal death and/or restoring neuronal function. Several classes of agents (including stimulators of glutathione reductase, inhibitors of monoamine oxidase, and iron chelators) may slow the progression of the disease (3). Serial studies with an agent that provides a quantitative measure of dopamine terminal innervation of striatum would be useful to evaluate the efficacy of such putative "neuroprotective" agents.

We have developed a promising single photon emission computed tomography (SPECT) radiotracer, [^{123}I](1*R*)-2β-carbomethoxy-3β-(4-iodophenyl)tropane ([^{123}I]β-CIT) (4) [also designated RTI-55 (5)], which labels the dopamine transporter. This protein is located in the presynaptic membrane and transports dopamine from the synapse back into the terminal. That is, [^{123}I]β-CIT labels sites located on the terminals of dopamine neuronal projections from the substantia nigra to the striatum and may, therefore, provide a measure of dopamine terminal innervation.

METHODS

SPECT imaging of [^{123}I]β-CIT was done in five patients with idiopathic Parkinson disease and five sex-matched healthy subjects; both groups had a similar mean age. All patients had symptoms that were responsive to L-dopa and had at least three of the following symptoms: resting tremor, bradykinesia, rigidity, and postural instability (Table 1). Treatment of the subjects with L-dopa was thought not to interfere with the imaging studies because animal experiments have shown that high doses of L-dopa (50 mg/kg i.v.) did not induce displacement of striatal [^{123}I]β-CIT activity (8). The healthy subjects (four males and one female; age 58 ± 6 yr, with these and subsequent data expressed as mean ± SEM) were taking no medications and were free of serious medical illnesses by physical examination and laboratory testing. All subjects gave written informed consent.

Four fiducial markers containing ≈7 μCi of ^{99m}Tc (1 Ci = 37 GBq) were attached to the skin along the canthomeatal line for realignment of all images from each subject in a plane parallel to the canthomeatal line. Subjects were injected i.v. with 13.5 ± 1.2 mCi of [^{123}I]β-CIT with a specific activity >5000 Ci/mmol and a radiochemical purity of >95%. Two serial scans of 5- to 10-min duration were typically obtained every 45 min for 6–8 hr on day 1; except for one patient, images of 15–30 min were obtained the following morning and/or afternoon.

SPECT images were acquired with the Ceraspect device (Digital Scintigraphics, Waltham, MA), which has a resolution in all three axes of 7.5–8 mm (full-width at half-maximum) measured with a point source in air. Images were acquired with a 20% symmetric window centered at 159 keV, reconstructed with a Butterworth filter (cutoff = 1 cm; power factor = 10), partially corrected for scatter with the manufacturer's software called septal penetration and displayed as 64 slices of 128 × 128 pixels (pixel size = 1.7 × 1.7 mm with an interslice distance of 1.7 mm). Attenuation correction was performed (μ

The publication costs of this article were defrayed in part by page charge payment. This article must therefore be hereby marked "*advertisement*" in accordance with 18 U.S.C. §1734 solely to indicate this fact.

Abbreviations: SPECT, single photon emission computed tomography; L-dopa, L-dihydroxyphenylalanine; β-CIT, (1*R*)-2β-carbomethoxy-3β-(4-iodophenyl)tropane; ROI, region of interest; PET, positron emission tomography.

‡To whom reprint requests should be addressed at: Diagnostic Radiology, TE-2, Yale University School of Medicine, P.O. Box 3333, New Haven, CT 06510.

Table 1. Characterization of patients

Patient	Sex	Age, yr	PD duration, yr	Medication, mg/24 hr: Dopa Sin	Dopa SinCR	Perg	Seleg	Aman	Neuroevaluation: H&Y	UPDRS: Total	UPDRS: Motor	Side
1	M	69	3		600			200	1	22.5	13	Right
2	M	40	8	200	800	2	10		3	29	19	Left
3	M	53	6	600		3	10		2.5	21	15	Left
4	F	62	2	450		2.25			2	42	28	Left
5	M	57	6	100	300		5		2	42	31	Left
Mean (± SEM)		56 (4.9)	5 (1.1)						2.1 (0.3)	31 (4.6)	21 (3.6)	

Demographic characteristics of patients include duration of Parkinson disease (PD) in years, medications [L-dopa as Sinemet (Sin), L-dopa as SinemetCR (SinCR), pergolide (Perg), selegiline (Seleg), and amantadine (Aman)], Hoehn and Yahr (H&Y) scale (6), Unified Parkinson's Disease Rating Scale (UPDRS) total and motor scales (7), and side of body with initial symptoms (Side). The neurological evaluation was done on the day before the SPECT scan. M, male; F, female.

= 0.15 cm^{-1}), and SPECT activity (cpm) was converted to absolute units of radioactivity (μCi) based upon a calibration factor (0.0069 μCi/cpm) determined from a cylindrical phantom of 20-cm diameter filled with an ^{123}I solution.

To better identify the brain anatomy, four of these subjects also had magnetic resonance imaging for coregistration with a total of 10 markers widely distributed around the head (9). The coregistered magnetic resonance and SPECT images were used to establish standard regions of interest (ROIs) for caudate, putamen, striatum (caudate plus putamen), and occipital lobe. Eight of the 64 SPECT slices with highest striatal activities were summed, and these standard ROIs (with preset area and shape) were visually positioned on the summed striatal slice. Occipital activity was almost identical to that in the cerebellum. The occipital ROI was selected because one subject did not have brain images that extended inferiorly to the cerebellum, but all subjects had images through the occipital lobe.

Plasma samples from the radial artery were used to measure the level of free parent compound separated from radiolabeled metabolites (10). Plasma concentration data were fit to a three-exponential function with weighted least-squares regression. Plasma clearance was calculated as the total dose divided by the area under the curve of the triexponential function. Plasma measurements from one healthy subject were technically flawed and could not be used.

Regional brain data were expressed in four ways: (*i*) normalized uptake calculated as brain activity (μCi/cm^3) divided by the injected dose (μCi) and the subject's body weight (g); (*ii*) ratio of activity in the target ROI to that in the occipital lobe; (*iii*) volumes of distribution of striatal activity [calculated as the unitless ratio at time (t) of striatal activity to the concentration of free parent tracer in plasma]; and (*iv*) graphical analysis (or so-called Patlak plot) of the striatal volume of distribution vs. effective exposure time, which equals $\int C_p(t)dt/C_p(t)$, where C_p is the concentration of free parent tracer in plasma. The slope of the Patlak plot has a hyperbolic relationship with the density (B_{max}) of target sites (11). The Patlak slopes of all healthy human subjects studied to date with [^{123}I]β-CIT have shown a curvilinear portion for the initial 80–120 min, which is followed by a segment that is fairly linear by visual inspection (see Fig. 2*A*). Therefore, we have prepared Patlak graphs and calculated the slope of results from day 1 with the exclusion of data from the initial 200 min of effective exposure time (θ), which corresponded to 106 ± 4 min real time.

RESULTS

As expected from its low mass dose, the injection of [^{123}I]β-CIT induced no subjective effects in any of the 10 volunteers. Brain activity was highly concentrated in striatal regions (Fig. 1). Striatal activity in all healthy subjects increased during the 6- to 8-hr scanning session on day 1 and showed an additional increase in the first scan acquired on day 2 (Fig. 2 and Table 2). In contrast, striatal activity from the Parkinsonian patients generally peaked by 3- to 4-hr after tracer injection and showed similar values on day 2 compared with the last scan of day 1.

The plasma clearance of the free parent tracer in the Parkinsonian patients (374 ± 67 liters/hr) was not significantly different ($P > 0.15$, unpaired Student's t test) from that in the healthy subjects (241 ± 24 liters/hr). Using a brain region thought to represent nonspecific uptake, the normalized levels of occipital uptake (μCi per cm^3/μCi per g) from the last scan on day 1 did not differ significantly in Parkinsonian patients (2.3 ± 0.3) compared with the healthy subjects (2.1 ± 0.7; $P > 0.7$).

The levels of striatal activity were compared at a time on day 1 (247–265 min) when scans had been acquired for all 10 subjects and again on day 2 (at 1390 ± 97 min for healthy subjects and 1270 ± 48 min for the patients). The outcome measures obtained from both days (normalized striatal activity, ratio to occipital activity, and distribution volume) were decreased in the Parkinsonian patients to 50–70% of those in control subjects. These differences became even more evident on day 2, at which time these outcome measures were 25–45% of uptake in healthy subjects (Table 2 and Fig. 3). The Patlak slope (which is calculated from data on only day 1) was reduced to ≈35% of control values.

For each of the four outcome measures, we performed a two-way ANOVA to examine the factors of patient vs. healthy groups ($P < 0.01$) and ROI differences in caudate vs. putamen ($P < 0.05$ for two of the outcome measures; Table 2) with a repeated measure on day 1 vs. day 2 ($P < 0.0001$). A significant interaction between day and subject group ($P < 0.05$) reflected the enhanced differences between patients and healthy subjects on day 2 compared with day 1.

Patients showed lateralized differences in brain activity, which was lower for each subject when using any of the four

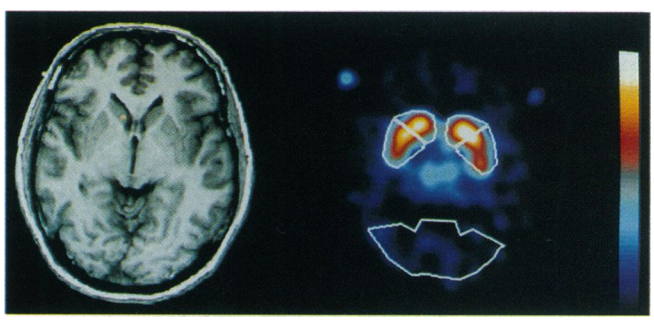

FIG. 1. Coregistered magnetic resonance (*Left*) and SPECT [^{123}I]β-CIT (*Right*) images from a healthy subject no. 3, showing the standard ROIs that were subsequently applied to all SPECT images from all subjects. Levels of SPECT activity are color-encoded from low (black) to high (yellow/white).

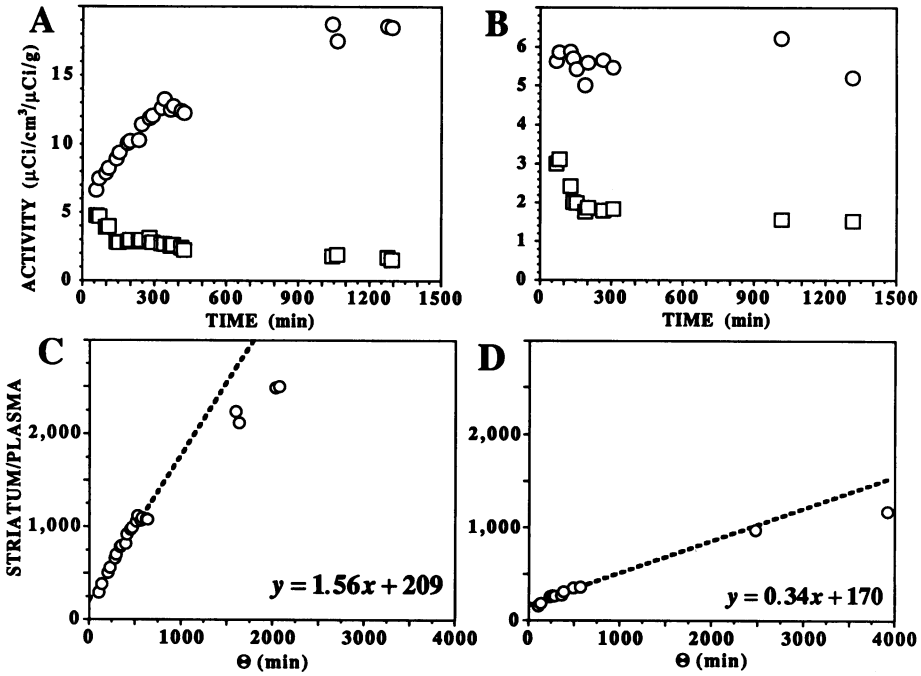

FIG. 2. (*A* and *B*) Time–activity curves. Normalized activity (μCi per cm^3/μCi per g) of average striatum (○) and occipital lobe (□) are plotted vs. time after injection of [^{123}I]β-CIT in a 42-yr-old healthy subject (*A*), and a 40-yr-old Parkinsonian patient (*B*). Note expanded scale on *y* axis in *B*. (*C* and *D*) Patlak plots of striatal activity. Patlak plots of average striatal activities from the same subjects as above: healthy subject (*C*) and Parkinsonian patient (*D*). The *y* axis represents the ratio of concentration of striatal activity (μCi/cm^3) at time *t* to concentration of free parent tracer in plasma (μCi/cm^3) at time *t*; i.e., $C_p(t)$. The *x* axis (effective exposure time θ) is given by $\int C_p(t)dt/C_p(t)$.

outcome measures in the striatum contralateral to the side of the body with the initial presentation of symptoms (Table 3).

To examine whether patients showed differential losses in the striatal subregions, we calculated the ratio of putamen to caudate activity. For all outcome measures except the Patlak slope, patients had significantly lower ratios than healthy subjects, consistent with a larger percentage loss of dopamine transporters in putamen than in caudate. For measures of normalized activity, ratio to occipital activity, and distribution volume, the statistical significance of patients vs. healthy subjects was $P < 0.01$ on day 1 and $P < 0.005$ on day 2 (two-tailed *t* test).

To examine whether the decreased brain uptake in the patients could merely be due to decreased striatal blood flow, we examined the distribution volumes of striatal activity at early and late times because the effects of flow should be evident on early images. In fact, the distribution volumes of mean left and right striatal activity were not significantly different in early images but increasingly diverged by the last scan of day 1. These ratio results for patients and healthy subjects, respectively, were as follows: 190 ± 22 vs. 230 ± 53 at 72 ± 1 min, $P > 0.4$ and 350 ± 32 vs. 610 ± 110 at 260 ± 2.7 min, $P < 0.04$.

DISCUSSION

The major finding of this study is that patients with Parkinson disease can be clearly distinguished from healthy subjects relative to SPECT measurements of brain uptake of [^{123}I]β-CIT. The decrease of the four different outcome measures

Table 2. Measurements of activity in caudate and putamen

	Day 1			Day 2			ANOVA,† *P*			
Measure*	*n*	Caudate	Putamen	*n*	Caudate	Putamen	Group	Region	Day	Group–day
Parkinson										
Activity	5	8.1 ± 0.8	5.8 ± 0.4	4	10.1 ± 1.3	4.9 ± 1.0	0.0001	0.05	0.0001	0.0001
Ratio to occip	5	3.6 ± 0.2	2.7 ± 0.3	4	5.4 ± 0.5	2.6 ± 0.5	0.0001	0.01	0.0001	0.0001
Distribution vol	5	420 ± 43	300 ± 28	4	1400 ± 430	760 ± 290	0.01	NS	0.0001	0.05
Patlak slope	5	0.5 ± 0.1	0.3 ± 0.04				0.0001	NS		
Healthy										
Activity	5	9.8 ± 0.9	9.5 ± 0.7	5	19 ± 1.3	15 ± 1.7				
Ratio to occip	5	5.0 ± 0.7	4.9 ± 0.6	5	13 ± 0.6	11 ± 1.0				
Distribution vol	4	630 ± 120	600 ± 100	4	2500 ± 500	2100 ± 540				
Patlak slope	4	1.2 ± 0.2	0.9 ± 0.1							

*Activities in caudate and putamen (mean values of right and left sides) were measured on day 1 (255 ± 2 min) and day 2 (1330 ± 56 min). Outcome measures (means ± SEMs) were as follows: activity (μCi per cm^3/μCi per g) normalized to injected dose and body weight; ratio to occip (unitless ratio of striatal-to-occipital activity); distribution vol (unitless ratio of striatal activity to the concurrent concentration of the plasma free parent tracer); Patlak slope [min^{-1}; slope of linear fit of Patlak plots from data acquired on day 1 excluding the initial data points within the first 200 min of effective exposure time (θ)].

†*P* values are listed for statistical analyses with a two-factor ANOVA (patient vs. healthy groups and caudate vs. putamen regions) and a repeated measure on day 1 vs. day 2. A significant interaction between group and day (Group–day) reflects the enhanced differences between patients and healthy subjects on day 2 in comparison with day 1. NS, not significant ($P > 0.05$).

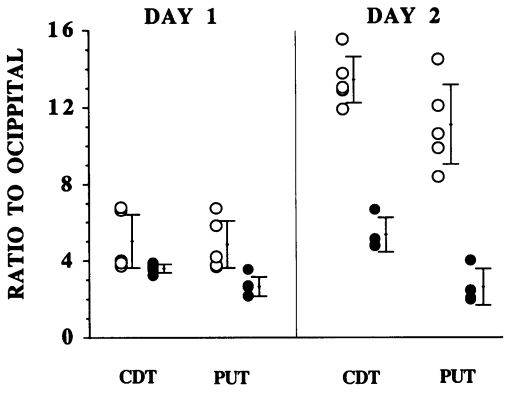

FIG. 3. Ratio of activity in caudate (CDT) and putamen (PUT) to that in occipital lobe in healthy subjects (○) and patients (●) on day 1 (255 ± 2 min) and day 2 (1330 ± 56 min). Error bars indicate means ± 2 SEMs, which approximate a 95% confidence interval.

(with an approximate range of 55–75%) in the patient group is not as great as the loss of endogenous dopamine reported in postmortem human tissue samples (>80%) (1). However, the patients in the present study (Hoehn and Yahr stages 1–3) appear much less severely affected than those from postmortem examinations. Because of the significant interval of values we find between symptomatic patients and healthy subjects, our data suggest that *in vivo* imaging may be able to identify patients before the development of definitive clinical symptoms.

Selection of Outcome Measures. Four different outcome measures (normalized activity, volume of distribution, Patlak slope, and striatal-to-occipital ratio) were selected because each provides a different view of the results. The normalized uptake is perhaps the most straightforward and reflects the percentage of the injected dose taken up by the striatum. However, this measurement does not correct for variations in peripheral clearance between subjects. The volume of distribution expresses brain activity relative to the simultaneously measured level of free parent tracer in plasma. Thus, this measurement partially corrects for intersubject variability in the rates of peripheral tracer clearance. However, the volume of distribution is the ratio of brain-to-plasma activity at only one time point and does not completely compensate for variations in clearance before the time of measurement. In contrast, the graphic analysis or so-called Patlak plot assesses a full-time course of brain activities relative to multiple measurements of plasma activity (i.e., the input function). Among the outcome measures studied, the Patlak plot is intended to provide the most thorough analysis with potentially complete compensation for variations in tracer clearance. However, these three outcome measures would all be difficult to apply in routine clinical studies: all require calibration of the camera relative to the administered dose, and both the volume of distribution and Patlak plot require metabolite-corrected plasma measurements.

The ratio of striatal-to-occipital activity is the simplest measure and would be the easiest to apply in clinical studies. This ratio requires neither calibration of the camera relative to injected dose nor any plasma measurements. We are uncertain at present which of these four values is the most accurate measurement to apply in future studies of Parkinsonian patients. However, we have recently completed serial image acquisitions in four young healthy subjects on day 2 and found very stable radioactivity levels in striatum and occipital lobe over an 8-hr period (changing by ≈1–3% per hr). These results suggest, at least, that healthy subjects will have a stable striatal-to-occipital ratio which could be measured at almost any convenient time on day 2. However, this ratio provides a measure linearly related to the density of target sites only at equilibrium.

Time-Related Differences. Compared with results from day 1, SPECT imaging on day 2 showed greater differences between healthy subjects and Parkinsonian patients, which would be consistent with a loss of target sites in this disorder. Brain uptake of [^{123}I]β-CIT appears limited by its delivery to target sites in the striatum and shows slow accumulation for up to 8–15 hr in healthy subjects. Because no active or facilitated transport process has been identified, [^{123}I]β-CIT is presumed to cross the blood–brain barrier by passive diffusion with the direction and rate determined by the relative concentrations of free tracer in brain and plasma. At times earlier than 8–15 hr, the many striatal target sites in healthy subjects bind the tracer and maintain lower free-tracer levels in brain than in plasma. A transitory state of equilibrium is then achieved when the free-tracer level in brain is equal to the declining plasma tracer value, and no net uptake occurs. In comparison with healthy subjects, the reduced number of target sites in the Parkinsonian striatum presumably bind less tracer, yielding higher free-tracer levels in brain, and, therefore, showing an earlier time to transient equilibrium. These results are consistent with the more general principle that, when uptake of tracer is limited by delivery to target sites, peak uptake will occur earlier in areas with fewer sites. Thus, striatal activity peaked earlier in Parkinsonian patients than in healthy subjects. Differences between the two groups increased over time because values in healthy subjects continued to increase after peak values were reached in the patients.

Tomographic Imaging—Positron Emission Tomography (PET) Vs. SPECT. Functional brain imaging with SPECT and PET provides methods of high sensitivity to measure *in vivo* neurochemistry. SPECT technology offers several advantages in comparison with PET. PET radionuclides have short half-lives (e.g., ^{11}C, $t_{1/2}$ 20 min) and must be produced with an on-site cyclotron. In contrast, SPECT radionuclides have longer half-lives (e.g., ^{123}I, $t_{1/2}$ 13 hr) and can be commercially supplied. Furthermore, the resolution of SPECT devices has improved significantly in the last few years. The resolution of the SPECT camera used here is 7.5- to 8-mm full-width at half-maximum in all three axes measured in air, which compares favorably with that of commercially available PET devices (≈5 mm).

Three major technical advantages of PET over SPECT are (*i*) effective correction for tissue attenuation by means of a transmission scan; (*ii*) rejection of scatter radiation, and (*iii*) higher sensitivity. Nevertheless, techniques are available in SPECT to address these issues. Attenuation can be corrected in imaging of the head by assuming uniform photon attenuation equal to that of water in an ellipse drawn around the brain image, scatter radiation can be corrected by subtracting a scatter window, and the lower sensitivity of SPECT is partly compensated by the exceptionally high brain uptake of [^{123}I]β-CIT (12–14% of injected dose in human subjects; unpublished data).

6-[^{18}F]Fluoro-L-3,4-dihydroxyphenylalanine has been successfully used in animal and human studies to provide a measure of dopamine terminal innervation of the striatum. These studies have demonstrated decreased striatal uptake in Parkinsonian patients compared with healthy subjects (12). Furthermore, these studies have questioned the widely held notion that symptoms develop only after 85–90% depletion of endogenous dopamine levels. Imaging studies of patients with early signs of the disorder suggest symptoms may begin with only a 50–60% decrease in striatal dopamine terminal innervation (13).

After injection of 6-[^{18}F]fluoro-L-3,4-dihydroxyphenylalanine in primates, the majority of striatal activity represents a combination of [^{18}F]fluorodopamine and the metabolite

Table 3. Lateralized uptake of striatal activity (day 1)

Measure	*n*	Contra	Ipsi	Ratio	Paired *t* test, *P*
Parkinson					
Activity	5	6.3 ± 0.6	7.2 ± 0.6	0.88 ± 0.05	<0.05
Ratio to occip	5	2.8 ± 0.1	3.3 ± 0.3	0.85 ± 0.07	<0.01
Distribution vol	5	330 ± 28	370 ± 34	0.88 ± 0.05	<0.05
Patlak slope	5	0.27 ± 0.09	0.47 ± 0.6	0.52 ± 0.14	<0.01
Healthy					
Activity	5	9.4 ± 0.8	9.8 ± 0.7	0.96 ± 0.02	NS
Ratio to occip	5	4.8 ± 0.7	5.0 ± 0.6	0.98 ± 0.01	NS
Distribution vol	4	600 ± 110	620 ± 100	0.96 ± 0.03	NS
Patlak slope	4	0.99 ± 0.12	1.04 ± 0.15	0.96 ± 0.05	NS

In the patient group, striata were identified as either contralateral (Contra) or ipsilateral (Ipsi) to the side of the body with initial symptom onset. Because the healthy group had no symptoms, contralateral and ipsilateral striata were arbitrarily identified as right and left, respectively. The ratio of contralateral to ipsilateral activities is indicated. See Table 2 legend for definitions of measures and units. Values represent means ± SEM. For each outcome measure, a paired *t* test was used to compare contralateral and ipsilateral values.

[^{18}F]fluoro-3-methoxydopamine (14). Thus, quantitation of the imaging results is not definitive, in part because of the radiolabeled metabolites present in striatum.

Imaging the Dopamine Transporter. Several radiotracers for the dopamine transporter have been developed: [^{11}C]cocaine, [^{11}C]nomifensine, [^{11}C]2β-carbomethoxy-3β-(4-fluorophenyl)tropane (CFT; also designated WIN 35,428), [^{123}I]β-CIT, and [^{18}F]GBR 13,119 (4, 5, 15–17). [^{18}F]GBR 13,119 and [^{11}C]nomifensine have relatively high nonspecific uptake. Radiolabeled cocaine may be particularly useful for studying the pharmacokinetics of the parent compound but has the limitations of relatively high nonspecific binding and rapid uptake and clearance from the brain. In comparison with cocaine, the analogs 2β-carbomethoxy-3β-(4-fluorophenyl)-tropane and β-CIT have higher affinity (≈10- and 150-fold, respectively), lower nonspecific binding, and slower brain kinetics. Although β-CIT has high affinity for both dopamine and 5-hydroxytryptamine transporters, the vast majority (i.e., >95%) of striatal activity of i.v. administered [^{123}I]β-CIT appears to be associated with the dopamine transporter (8).

Summary. The diagnosis of Parkinson disease remains a clinical judgment based primarily upon motor examination and the patient's response to L-dopa. Recent data correlating clinical impression with subsequent pathology showed only 75–80% agreement between clinical and pathological diagnoses (18). Our preliminary results suggest that [^{123}I]β-CIT is a marker for the striatal loss of dopamine transporters in Parkinsonian patients. Thus, given the relatively wide availability of SPECT technology, [^{123}I]β-CIT is a promising research and potentially clinical agent that may help diagnose Parkinson disease in its early stages, to monitor progression of the disease, to assess the efficacy of agents believed to slow progression of the disease, and to distinguish the idiopathic disorder from other Parkinsonian syndromes (like striatonigral degeneration) with more widespread pathology.

We gratefully acknowledge E. O. Smith and G. Wisniewski for expert assistance as nuclear medicine technologists and E. Lerner for statistical analyses. This work was supported by gifts from Nihon Medi-Physics Co., Ltd. (Tokyo); Rose and Philip Hoffer; and funds from the National Parkinson's Foundation, the Department of Veterans Affairs (Substance Abuse Research Fellowship to B.E.S.), and the National Institute of Mental Health (R43-MH48243).

1. Kish, S. J., Shannak, K. & Hornykiewicz, O. (1988) *N. Engl. J. Med.* **318,** 876–880.
2. Kaufman, M. J. & Madras, B. K. (1991) *Synapse* **49,** 43–49.
3. Parkinson's Study Group (1992) *N. Engl. J. Med.* **328,** 176–183.
4. Neumeyer, J. L., Wang, S., Milius, R. A., Baldwin, R. M., Zea-Ponce, Y., Hoffer, P. B., Sybirska, E., Al-Tikriti, M., Charney, D. S., Malison, R. T., Laruelle, M. A. & Innis, R. B. (1991) *J. Med. Chem.* **34,** 3144–3146.
5. Shaya, E. K., Scheffel, U., Dannals, R. F., Ricaurte, G. A., Carroll, F. I., Wagner, H. N., Jr., Kuhar, M. J. & Wong, D. F. (1992) *Synapse* **10,** 169–172.
6. Hoehn, M. M. & Yahr, M. D. (1967) *Neurology* **17,** 427–442.
7. Fahn, S., Elton, R. & Members of the Unified Parkinson's Disease Rating Scale Development Committee (1987) in *Recent Developments in Parkinson's Disease*, eds. Fahn, S., Marsden, C., Calne, D. & Goldstein, M. (Macmillan Healthcare Information, Florham Park, NJ), Vol. 2, pp. 153–164.
8. Laruelle, M., Baldwin, R. M., Malison, R. T., Zea-Ponce, Y., Zoghbi, S. S., Al-Tikriti, M. S., Sybirska, E. H., Zimmermann, R., Wisniewski, G., Neumeyer, J. L., Milius, R. A., Wang, S., Smith, E. O., Roth, R. H., Charney, D. S., Hoffer, P. B. & Innis, R. B. (1993) *Synapse* **13,** 295–309.
9. Malison, R. T., Miller, E. G., Greene, R., McCarthy, G., Charney, D. S. & Innis, R. B. (1993) *J. Comput. Assist. Tomogr.* **17,** 952–960.
10. Baldwin, R. M., Zea-Ponce, Y., Zoghbi, S. S., Laruelle, M., Al-Tikriti, M. S., Sybirska, E. H., Malison, R. T., Neumeyer, J. L., Milius, R. A., Wang, S., Stabin, M., Smith, E. O., Charney, D. S., Hoffer, P. B. & Innis, R. B. (1993) *Nucl. Med. Biol.* **20,** 597–606.
11. Patlak, C. S. & Blasberg, R. G. (1985) *J. Cereb. Blood Flow Metab.* **5,** 584–590.
12. Calne, D. B., Langston, J. W., Martin, W. R. W., Stoessl, A. J., Ruth, T. J., Adam, M. J., Pate, B. D. & Schulzer, M. (1985) *Nature (London)* **317,** 246–248.
13. Leenders, K. L., Salmon, E. P., Tyrrell, P., Perani, D., Brooks, D. J., Sager, H., Jones, T., Marsden, D. & Frackowiak, R. S. J. (1990) *Arch. Neurol.* **47,** 1290–1298.
14. Garnett, E. S., Firnau, G., Nahmias, C. & Chirakal, R. (1983) *Brain Res.* **280,** 169–171.
15. Aquilonius, S.-M., Bergstrom, K., Eckernas, S.-A., Hartvig, P., Leenders, K. L., Lundquist, H., Antoni, G., Gee, A., Rimland, A., Uhlin, J. & Langstrom, B. (1987) *Acta Neurol. Scand.* **76,** 283–287.
16. Fowler, J. S., Volkow, N. D., Wolf, A. P., Dewey, S. L., Schlyer, D. J., MacGregor, R. R., Hitzemann, R., Logan, J., Bendriem, B., Gatley, S. J. & Christman, D. (1989) *Synapse* **4,** 371–377.
17. Kilbourn, M. R., Carey, J. E., Koeppe, R. A., Haka, M. S., Hutchins, G. D., Sherman, P. S. & Kuhl, D. E. (1989) *Nucleic Med. Biol.* **16,** 569–576.
18. Rajput, A., Rodzilsky, B. & Rajput, A. (1991) *Can. J. Neurol. Sci.* **18,** 275–278.